International Journal of Mechanical, Industrial and Aerospace Sciences
ISSN: 2517-9950
Vol:3, No:4, 2009

Loop Heat Pipe: Simple Thermodynamic

Mohammad Hamdan, and Emad Elnajjar

***Abstract*—**The LHP is a two-phase device with extremely high effective thermal conductivity that utilizes the thermodynamic pressure difference to circulate a cooling fluid. A thermodynamics analytical model is developed to explore different parameters effects on a Loop Heat Pipe (LHP).. The effects of pipe length, pipe diameter, condenser temperature, and heat load are reported. As pipe length increases and/or pipe diameter decreases, a higher temperature is expected in the evaporator.

***Keywords*—**Loop Heat Pipe, LHP, Passive Cooling, Capillary Force.

NOMENCLATURES

A	wick cross sectional area, m^2
C_p	specific heat capacity of the liquid, *kJ/kg.K*
CPL	Capillary pumped loop
CPS	Coherent Porous Silicon
h	enthalpy, *KJ/kg*
h_{cc}	convection coefficient in the compensation chamber, W/m^2K
k	thermal conductivity, *W/m.K*
ℓ	pipe length, *m*
L	wick thickness, *m*
LHP	loop heat pipe
M	mass, *kg*
$\dot{m}$	mass flow rate, *kg/s*
P	pressure, *Pa*
Q	heat flow, *W*
R	pipe radius, *m*
T	temperature, *K*
V	volume, m^3
x	quality
Greek symbols	
ρ	density, kg/m^3
μ	dynamic viscosity, *kg/s.m*
ε	porosity (0 to 1)
σ	surface tension, *N/m*
β	volumetric ratio (0 to 1), $\frac{V_{v,cc}}{V_{cc}}$
Subscript:	
1	Upper surface of the wick
2	Inlet of condenser
3	Vapor interface in the condenser
4	Liquid interface in the condenser
5	Condenser outlet
6	Compensation chamber inlet
c	condenser
cc	Bottom surface of the wick
cc,sat	Compensation chamber saturation conditions
e	evaporator
eff	Effective
l	Liquid
s	solid
sat	Saturated condition
v	Vapor
w	wick

I. INTRODUCTION

ONE of the biggest limitation facing the electronic industry is the availability of an efficient unconventional cooling system which can steadily get read of the generated heating loads of these electronics. Different methods have been utilized to provide better cooling techniques. One of the heavily investigated approaches involves cooling by integrating loop heat pipe (LHP) into the electronic components package. The LHP utilizes the interfacial force to direct the flow and the thermodynamic force to pump the cooling fluid from the evaporator to the condenser. Satellite manufacturers are interested in such cooling device where no pump is needed and the system is self-circulating, i.e. the system use passive forces to circulate the flow. Having no pump in space applications will reduce the launching price tag and the preservation cost. Scientists try to utilize the passive

forces in the liquid such as thermodynamic effect, capillary effect, osmotic effect, viscosity effect, and expansion effect to create such self-circulating system. The possibility of using LHP cooling technique is started appearing in other common devices such as air-conditioning [2], heat exchanger [3], and heat recovery components.

The LHP starts essentially with applying heat load at the evaporator where vapor starts to develop and temperature starts to rise. The temperature difference between the evaporator and the condenser works as a thermodynamics pump allowing the circulation of the cooling fluid while the interfacial interface direct the flow in the preferred direction. The evaporated liquid in the evaporator starts to move toward the condenser side through the vapor line since the other line, liquid line, is blocked by the vapor-liquid interface in the CPS wick. The interface will hold the pressure preventing any back flow and at the same time providing uninterrupted liquid flow. Hence, the circulated working fluid carries the heat away from the evaporator to the condenser.

Investigating the LHP performance includes many different parameters such as working fluid, optimum wick pore size, working temperature and pressure, evaporator wick properties and design. Chernysheva et al. [4] investigated different modes of the LHP and the effect of cooling fluid distribution in the LHP. Chandratilleke et al. [5] investigated four different working fluids trying to develop a loop heat pipe that can work in a cryogenic temperature range of 4 to 77 K. Also, Chandratilleke et al. [5] showed that the loop heat pipe was able to transport at least 10 times the amount of heat as compared to a solid copper rod of the same size. A diameter optimization was presented by Hölke et al. [6] for a micro coherent porous silicon wick using water as the working fluid. Hölke et al. [6] showed that an effective way to increase the loop heat pipe's performance is by reducing the pressure drop in the evaporator.

The first patent related to a LHP was issued in the United State of America to Maidanik et al. in 1985 [7]. It is observed that very few theoretical and experimental LHP models are available in the literature. This is due to (1) the complexity of phase change, (2) the different phenomena related to LHP, and (3) the limited amount of data that has been published. Phase change occurs by different mechanisms depending upon many factors such as the temperature difference between the fluid and the hot surface, the surface structure, the gravity, and the fluid pressure. These factors are discussed in different places in the literature and will not be covered here [8]. Many different phenomena related to the LHP which have appeared in the experiments, still need more study and analysis. These phenomena are bubble formation in the compensation chamber, interface oscillation, and wick dry out.

It is important for the LHP designer to know the difference between the capillary pumped loop (CPL) and the LHP. The differences between these two systems are discussed by Nikitkin and Cullimore [9]. The major arrangement design difference is the position of the compensation chamber. In a LHP, the compensation chamber is directly attached to the evaporator while in a CPL the compensation chamber is connected to the evaporator through a piping system. This design difference results in a LHP being more robust and simpler to start.

The effect of leak heat from the LHP evaporator was firstly introduced by Hamdan et al. [10] and Hoang et al. [11]. In this paper, authors found that the amount of leak heat is a critical design parameter and it is function of the convection coefficient in the compensation chamber.

A model of the steady state behavior of the LHP can be found in Kaya [12]. Kaya presents a mathematical steady state model for the LHP with an experimental validation. Launay and Sartre [13] presented a review of recent activity in LHP and concluded that the difficulty of successful LHP parameterize model is due to the strong coupling between LHP parameters, therefore, in this paper the authors decide to utilize EES solver which will allow modeling with variable thermodynamics properties.

Most of the previous studies investigate the cylindrical evaporator geometry while this work presents a flat evaporator model [14]. The optimum parameters of a flat evaporator with Coherent Porous Silicon wick was presented by Hamdan [15]. A flat evaporator used by Cytrynowicz et al. [16, 17] is more convenient in electronic cooling than cylindrical evaporators that are studied more frequently.

II. Theoretical Modeling

A schematic diagram of the current LHP is presented in Fig. 1. A piecewise model is used to describe the entire loop including the five major components in the LHP, which are wicked evaporator, compensation chamber, condenser, vapor line, and liquid line. The physical dimensions of the current LHP are listed in Table I. More details about the CPS wick fabrication techniques or LHP packaging is presented in Cytrynowicz et al. [16, 17].

In order to simplify the problem, some assumptions are adopted as follows:

1) A piecewise steady state thermal model is presumed along the LHP.
2) The compensation chamber is at saturated mixture equilibrium conditions.
3) The liquid is leaving the compensation chamber as a single-phase liquid.
4) The vapor-liquid interface in the condenser is assumed to always remain at the condenser entrance. One can anchor the interface to the entrance of the condenser by enhancing the condenser performance or by introducing wick structure to the condenser.
5) The phase change occurs at a constant temperature and pressure.
6) The porous wick is fully wetted with liquid cooling fluid.
7) The vapor and liquid lines and the compensation chamber are insulated and contained single phase flow. Cimbala et al. [18] reported single phase is applicable for steady state.
8) The flow is laminar, incompressible, and at steady state.

9) Uniform heat flux is applied to the evaporator to assure no periodic flow phenomena [18]. No heat lost from the evaporator is counted since the study focus on actual amount of heat going to the cycle.

Continuity equation

The total mass inside the sealed LHP can be calculated by knowing the density distribution though the LHP which is written as follow:

$$M_{total} = M_{v,cc} + M_{l,cc} + M_{v,pipe} + M_{l,pipe} + M_e \quad (1)$$

$$M_{total} = \rho_{v,cc} V_{cc} \beta + \rho_{l,cc} V_{cc} (1-\beta) + \left(\frac{\rho_{v,c} + \rho_{v,e}}{2} \right) \pi r^2 \ell_v + \rho_{l,c} \pi r^2 (\ell - \ell_v) + \rho_{v,e} V_e \quad (2)$$

Where (β) is the volumetric ratio ($\frac{V_{v,cc}}{V_{cc}}$) and is determined by calculating vapor volume in compensation chamber to total volume of the compensation chamber ($\beta = 0.2$ is assumed in the current model). Volume ratio is the vapor space inside the compensation chamber to the total volume of the compensation chamber. The volume ration would be equal to the porosity of secondary wick if the CC was filled with the secondary wick which is not the case the current modeled LHP.

Momentum equation

The working fluid is circulated in the LHP from the evaporator to the condenser through the vapor line and back again to the evaporator through the liquid line. Due to the large latent heat of vaporization of water, a small amount mass flow rate is circulated in the LHP. The small flow rate with the small pipe diameter to length ratio justifies the assumption of laminar fully developed flow for both liquid and vapor flow. For laminar fully developed flow, the pressure losses in the liquid pipe and vapor pipe can be expressed as shown in equation (3) and equation (4), respectively. The effects of joints and bends are not considered in this model.

$$\Delta P_l = P_c - P_6 = \frac{8 \mu_{l,c} \dot{m} (\ell - \ell_v)}{\pi \rho_{l,c} R^4} \quad (3)$$

$$\Delta P_v = P_1 - P_c = \frac{8 \mu_{v,c} \dot{m} \ell_v}{\pi \left(\frac{\rho_{v,c} + \rho_{v,e}}{2} \right) R^4} \quad (4)$$

Energy equation

An energy balance is needed in the evaporator where heat is provided and at the condenser where heat is removed. The tube is insulated and the compensation chamber is at equilibrium. The total heat removed is defined by the following equation:

$$Q_{in} = \dot{m}(h_1 - h_6) \quad (5)$$

$$Q_{out} = \dot{m}(h_2 - h_5) \quad (6)$$

Since the LHP pipes are insulated, then for a steady state cyclic loop heat pipe the amount of heat leaving at the condenser should equal the amount of heat absorbed at the evaporator, Equation (7).

$$Q_{in} = Q_{out} \quad (7)$$

Thermodynamics relations

To find the solution of the conservation equations (1-7), closure thermodynamics relations are needed. The thermodynamics relations are at the saturation conditions of the evaporator and the condenser which are shown as follow:

$$h_1 = f(T_1, P_1, x_1) \quad (8)$$

$$h_6 = f(T_6, P_6, x_6) \quad (9)$$

$$h_1 = h_2 \quad (10)$$

$$h_5 = h_6 \quad (11)$$

Equations (1-11) are algebraic equations that can be solved for the unknowns using EES solver techniques. For the present LHP model, the four key independent design parameters are; (1) The total mass charge, (M), (2) The condenser temperature, (T_c), (3) The total heat removed by the LHP, (Q), and (4) the LHP geometry namely pipe diameter and length.

Pc is the condenser pressure which is saturate pressure. Therefore it is function of saturated temperature Tc. The LHP thermodynamics cycle consists of four main processes which are; (1) Constant pressure heat addition in the evaporator, (2) Constant enthalpy in the insulated liquid pipe, (3) Constant pressure heat rejection in the evaporator, and (4) Constant enthalpy in the insulated vapor pipe.

III. Results and Discussion

Schematics of the main components of the loop heat pipe is shown in Fig. 1. The results of the model were run for three constant condenser temperatures cases: 40, 60 and 80 ^{o}C. This study covers a range of steady state heat load of 10 to150 W. Fig. 2 presents the thermodynamics cycle of the loop heat pipe with a condenser temperature of 60 ^{o}C as produced by the model.

In the evaporator, the total heat removed is divided into three parts which are latent heat, sensible heat, and leak heat and are determined as follow:

$$Q_{in} = Q_{laten} + Q_{sensible} + Q_{leak} \quad (12)$$

$$Q_{latent} = \dot{m} h_{fg,e} \quad (13)$$

$$Q_{sensible} = \dot{m} C_l (T_{cc} - T_1) \quad (14)$$

$$Q_{leak} = h_{cc} A (T_{cc} - T_{cc,sat}) \quad (15)$$

The leak heat occurs between the bottom surface of the wick and the equilibrium compensation chamber and T_{cc} is calculated as follow, Hamdan et al. [10]

$$T_{cc} = T_h - \left(\frac{Q - \dot{m} h_{fg,c}}{\dot{m} C_{p,l,c}} \right) \left(1 - e^{-\frac{\dot{m} C_{p,l,c} L}{k_{eff} A}} \right) \quad (16)$$

Where k_{eff} is the effective thermal conductivity of the wick and is expressed as $k_{eff} = k_l \varepsilon + k_s (1 - \varepsilon)$, Kaviany [19].

Utilizing equations (13-16), the results of the ratio of the leak heat and the latent heat to the total heat are shown in Fig. 3. The charts shows that as heat load increase the ratio of the leak heat to the total heat increase while the ratio of the latent heat to the total heat decrease, this is due to the increase on the mass flow rate of cooling fluid which would enhance convection heat transfer to the compensation chamber. Also higher heat load will raise the evaporator temperature which will increase the leak heat to the compensation chamber.

The amount of leak heat is related to the convection heat transfer in the compensation chamber which modeled as thermal resistance. The convection coefficient, h_{cc}, is variable and changes with the mass flow rate and wick configurations. The results of the calculated convections heat transfer coefficient as function of heat load is shown in Fig. 4.

In order to have functional LHP without flow interruption, the compensation chamber needs to be in equilibrium state. To achieve the equilibrium state and to compensate for the heat leaking to the compensation chamber, a sub-cooled liquid need to be provided. The sub-cooled temperature needed is calculated as follow.

$$T_6 = T_{cc,sat} + \frac{Q_{leak}}{\dot{m} C_{p,l,cc,sat}} \quad (17)$$

From above model, the evaporator temperature (T_e) and the compensation chamber temperature T_{cc} are calculated. Also from equation (16) and (17) the compensation temperature and the sub-cooled temperature are calculated, respectively. These four temperatures are reported in Figs. 5-7 for three different condenser temperature settings. From Figs. 5-7, the evaporator temperature (top side of the wick) has close temperature as the bottom side of the wick and this due to high conductivity and low porosity ($\varepsilon = 20\%$) of the wick. As expected, as heat load increases a lower sub-cooled temperature (T_6) is needed. Figs. 5-7 indicate that for same heat load as condenser temperature increase from 40 ^{o}C to 80 ^{o}C, the temperature difference decrease. This can be explained by the fact that water saturation temperature to saturation pressure gradient decrease as saturation temperature increase, Fig. 8.

The maximum pressure that the interface can hold depends on the radius of curvature of the pores as well as the solid and fluid properties. It is obvious that point (1) will have the highest pressure in the loop while point (6) will have the minimum one. Also the quality of point (cc,sat) depends on the design sizing of the compensation chamber. The LHP compensation chamber sizing is very critical, Ku [20]. It is required to have the pressure difference between points (1) and (cc,sat) less or equal to the capillary pressure developed in the wick. Also, it is important to maintain point (6) at or below the saturation temperature in order to prevent any bubbles forming in the liquid line. From point (cc,sat) only liquid from the compensation chamber will start moving through the secondary wick to the primary wick.

Utilizing the present model, one can predict the optimum size for the piping system. Fig. 9 shows that having larger tube size is desirable to reduce the pressure drop. Most of the pressure drop occurred in the LHP is due to the vapor region which include the vapor tubes and the evaporator vapor cavity. A higher pressure drop in the pipe mean a higher pressure is needed in the evaporator to drive the working fluid. A higher pressure in the evaporator will lead to a higher temperature in the evaporator which is not desired. The vapor line length has an opposite effect, as the length get larger more pressure is needed to drive the vapor. This indicates that the evaporator temperature will increase with the pumping distance.

IV. Conclusion

The performance of a stable LHP was predicted using a simple steady state thermodynamic analytical model. The model used to optimize the LHP conditions: operational and geometrical. It is found that the leak heat from the evaporator due to temperature difference between the wick and the compensation chamber need to be balanced by a sub-cool liquid, otherwise a failure of the LHP operation is expected. This model is able to identify the sub-cooled fluid temperature required to accomplish a functional stable LHP and an equilibrium compensation chamber state. The model predicts that the pipe length to diameter ratio was directly proportional to evaporator temperature.

References

[1] Yu.F. Maydanik, Review Loop heat pipes, Applied Thermal Engineering, 25 (2005) 635–657.
[2] Alklaibi, A.M., Evaluating the possible configurations of incorporating the loop heat pipe into the air-conditioning systems, International Journal of Refrigeration (2008), doi:10.1016/j.ijrefrig. 2007.11.007

[3] L. L. Vasiliev, Review Heat pipes in modern heat exchangers, Applied Thermal Engineering, 25 (2005) 1–19
[4] Chernysheva M.A., Vershinin S.V., Maydanik Yu. F., Operating temperature and distribution of a working fluid in LHP, International Journal of Heat and Mass Transfer, 50 (2007) 2704–2713.
[5] Chandratilleke C., Hatakeyama H., and Nakagome H., Development of Cryogenic Loop Heat Pipes, Cryogenics, 38, 3, 263-269.
[6] Hoelke, H.T. Henderson, F. M. Gerner and M. Kazmierczak, Analysis of the Heat Transfer Capacity of a Micromachined Loop Heat Pipe, International Mechanical Engineering Congress and Exposition, IMECE, ASME Publication HTD-Vol. 364-3, 53-60, November 15-20, 1999, Nashville, Tennessee.
[7] Maidanik Y., Vershinin S., Kholodov V., and Dolggirev J., Heat Transfer Apparatus, US patent 4515209, May (1985).
[8] Dhir V., Kandlikar S., Fujita Y., Iida Y., and Heist R., Nucleate Boiling, Handbook of Phase Change: Boiling and Condensation, Editor Kandlikar S., Shoji M., and Dhir V., Ch. 4, pp 71-120, (1999).
[9] Nikitkin M., and Cullimore B., CPL and LHP Technologies: What are the Differences, What are the Similarities?, SAE Paper 981587, (1998).
[10] Hamdan, M., Gerner, F., Henderson, T., Steady State Model of a Loop Heat Pipe (LHP) With Coherent Porous Silicon (CPS) Wick in the Evaporator, The Nineteenth Annual IEEE Semiconductor Thermal Measurement and Management Symposium, pp 88-96, (2003).
[11] Hoang T. T., Ku J., Miniature Loop Heat pipes for Electronic Cooling, Proceedings of IPACK03, International Electronic Packaging Technical Conference and Exhibition, July 6-11, (2003), Maui, Hawaii, USA.
[12] Kaya T., Mathematical Modeling of Loop Heat Pipes and Experimental Validation, J. of Thermophysics & Heat Transfer, 13, 3, (1999), 314-320.
[13] Launay S., Sartre V., Parametric analysis of loop heat pipe operation: a literature review, Jocelyn Bonjour, International Journal of Thermal Sciences 46 (2007) 621–636.
[14] R. Singh et al., Operational characteristics of a miniature loop heat pipe with flat evaporator, International Journal of Thermal Sciences (2008), doi:10.1016/j.ijthermalsci.2007.12.013
[15] Hamdan M., Cytrynowicz D., Medis P., Shuja A.,Gerner F., Henderson H., Golliher E., Mellott K., Moore C., Loop Heat Pipe (LHP) Development by Utilizing Coherent Porous Silicon (CPS) Wicks, Proceedings of the 8th ITHERM Conference, May 29-June 2, (2002), 457-465.
[16] Cytrynowicz D., Hamdan M., Medis P., Shuja A.,Gerner F., Henderson H., Golliher E., Mellott K., Moore C., "MEMS Loop Heat Pipe Based on Coherent Porous Silicon Technology", Proceeding the Space Technology and Applications International Forum, (2002) 220-232 .
[17] Cytrynowicz, D., Hamdan, M., Medis, P., Henderson, T., Gerner, F., Golliher, E., "Test Cell for a Novel Planar MEMS Loop Heat Pipe Based on Coherent Porous Silicon", Space Technology and Applications International Forum, February 2 - 6, (2003), Albuquerque, New Mexico.
[18] J. M. Cimbala, J. S. Brenizer, Jr, A. Po-Ya Chuang, S. Hanna, C. T. Conroy, A.A. El-Ganayni, D. R. Riley, Study of a loop heat pipe using neutron radiography, Applied Radiation and Isotopes, 61 (2004) 701–705.
[19] Kaviany M., Principle of Heat Transfer in Porous Media, 2nd ed., Springer, New York, 1995.
[20] Ku J., "Operating Characteristics of Loop Heat pipes", 1999, 29th International Conference on Environmental system, Denver, Colorado, July 1999.

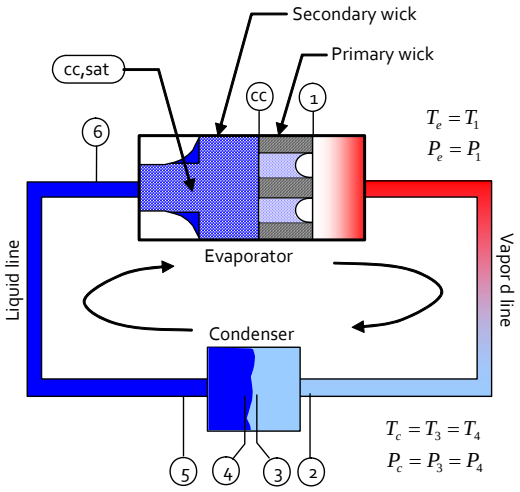

Fig. 1 A schematic diagram of the investigated loop heat pipe cycle

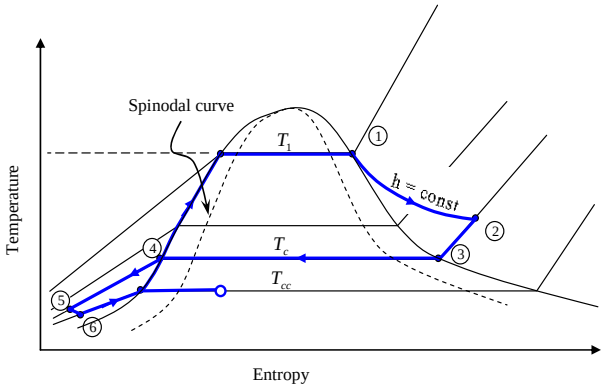

Fig. 2 A Temperature-Entropy thermodynamic diagram the investigated loop heat pipe cycle

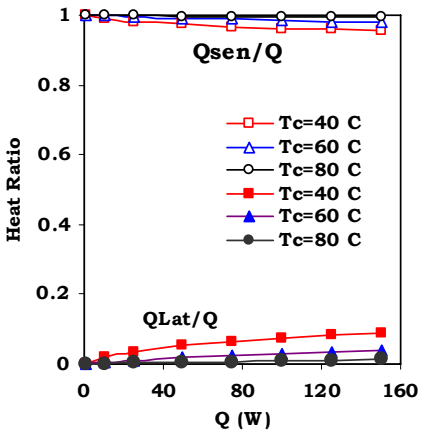

Fig. 3 The leak heat and the latent heat ratio relative to the total load Q

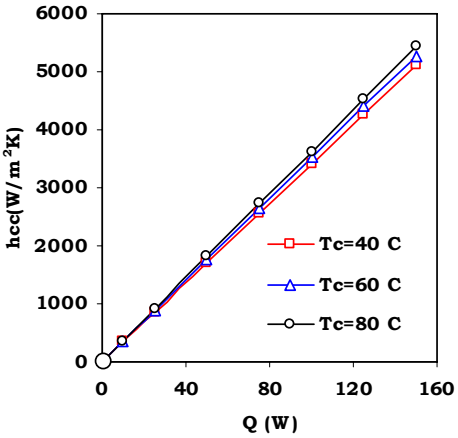

Fig. 4 The convection heat transfer coefficient as function of different heating loads, at different condenser temperature

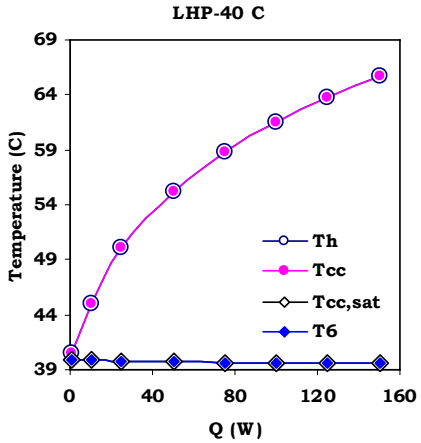

Fig. 5 The steady state temperature–total heat load performance curve at T_c = 40 C

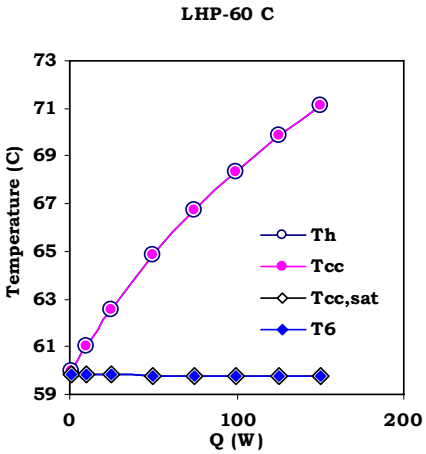

Fig. 6 The steady state temperature–total heat load performance curve at T_c = 60 C

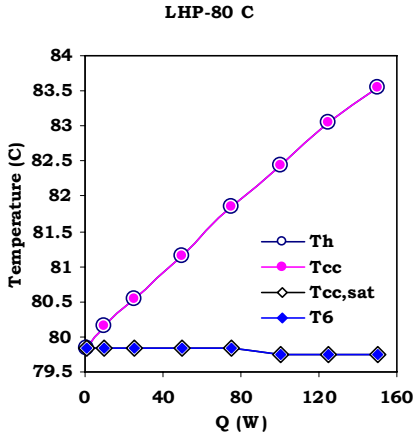

Fig. 7 The steady state temperature–total heat load performance curve at T_c = 80 C

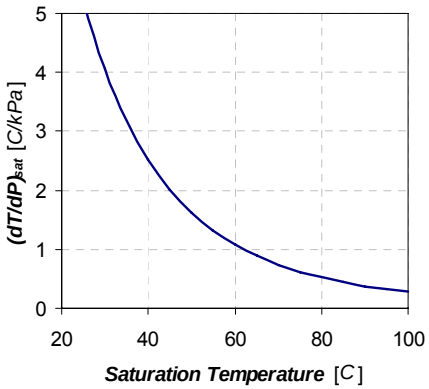

Fig. 8 The saturation temperature-pressure gradient as function of the saturation temperature

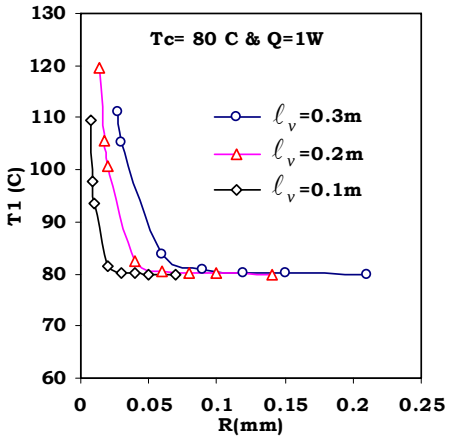

Fig. 9 The effect of vapor pipe size and tube length on the evaporator vapor temperature

TABLE I
THE DESIGN PARAMETERS FOR THE INVESTIGATED LOOP HEAT PIPE

Parameter	Value	Unit
Working fluid	Water	-
Evaporator:		
• Active area	1	cm^2
• Wick pore radius	2.5	*μm*
• Wick porosity	20%	-
• Wick Thickness	200	*μm*
• Silicon conductivity	140	*W/mK*
• Vapor cap depth	300	*μm*
Vapor line:		
• Diameter	0.7	*mm*
• Length	300	*mm*
Liquid line:		
• Diameter	0.7	*mm*
• Length	200	*mm*